

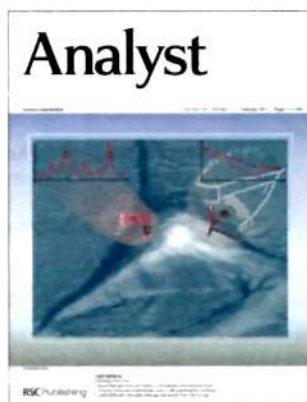
IN THIS ISSUE

ISSN 0003-2654 CODEN ANALAO 138(3) 713-964 (2013)



Cover

See Simon D. M. Jacques *et al.*, pp. 755–759.
Image reproduced by permission of Simon Jacques from *Analyst*, 2013, **138**, 755.



Inside cover

See Anhong Zhou *et al.*, pp. 787–797.
Image reproduced by permission of Anhong Zhou from *Analyst*, 2013, **138**, 787.

EDITORIAL

729

Rayleigh, Ramsay, Rutherford and Raman – their connections with, and contributions to, the discovery of the Raman effect

Robin J. H. Clark*

The key contributions of the four great Nobel Laureates – Lord Rayleigh, Sir William Ramsay, Lord Rutherford and Sir Chandrasekhara Raman – to the understanding of light scattering, to the identification and classification of the rare gases, and to the discovery in 1928 of the Raman effect are outlined.



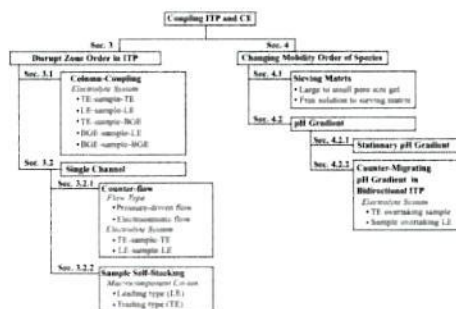
TUTORIAL REVIEW

735

Coupling isotachopheresis and capillary electrophoresis: a review and comparison of methods

Supreet S. Bahga and Juan G. Santiago*

We present a comprehensive review and comparison of the methodologies for increasing sensitivity and resolution of capillary electrophoresis (CE) using online transient isotachopheresis (tITP). We categorize and discuss the diverse set of coupled tITP and CE (tITP-CE) methods based on their fundamental principles for disrupting ITP and triggering CE.



755

A laboratory system for element specific hyperspectral X-ray imaging

Simon D. M. Jacques,* Christopher K. Egan,* Matthew D. Wilson, Matthew C. Veale, Paul Seller and Robert J. Cernik*

A method to look inside and through objects that provides images containing chemical information.

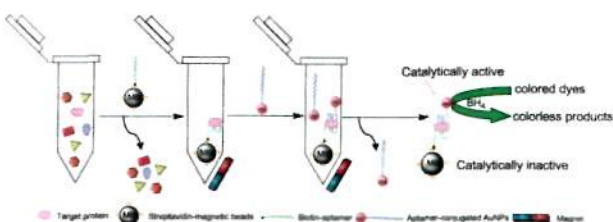


760

Enzyme-free colorimetric bioassay based on gold nanoparticle-catalyzed dye decolorization

Wei Li, Jie Li, Weibing Qiang, Jingjuan Xu and Danke Xu*

A novel, enzyme-free and aptamer-based colorimetric platform for protein detection has been developed, which takes advantage of aptamer-functionalized magnetic beads (MBs) for target capture, concentration and separation, and aptamer-conjugated gold nanoparticle (AuNP)-catalyzed color bleaching reaction of methyl orange (MO) to generate the colorimetric signals.

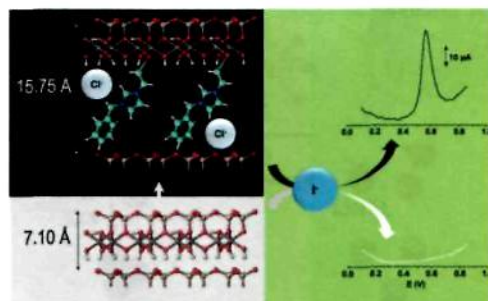


767

Ionic liquid-kaolinite nanohybrid materials for the amperometric detection of trace levels of iodide

Gustave Kenne Dedzo and Christian Detellier*

A modified kaolinite with anion exchange properties was successfully used for the amperometric quantification of iodide in aqueous solution.

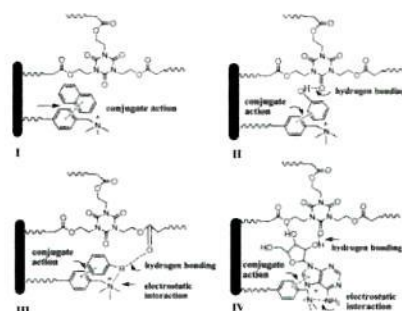


771

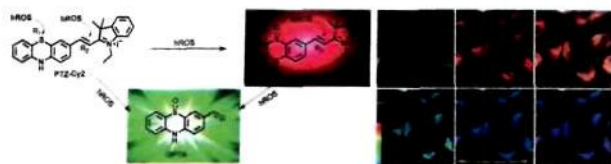
A facile versatile polymeric monolith for multiple separations

Xucong Lin,* Jia Lin, Yingying Sun, Yanping Li and Zenghong Xie*

A hydrophilic versatile polymeric monolith with hydrogen-bonding, π - π and electrostatic interactions, was developed by a simple "one-step" *in situ* polymerization. Excellent separation capabilities of various nonpolar and polar analytes were successfully achieved for multiple separations.



775

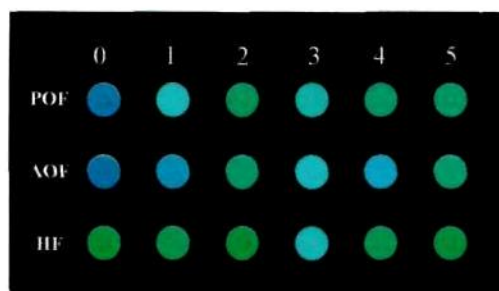


A novel fluorescent sensor for detection of highly reactive oxygen species, and for imaging such endogenous hROS in the mitochondria of living cells

Fei Liu, Tong Wu, Jianfang Cao, Hua Zhang, Mingming Hu, Shiguo Sun, Fengling Song, Jiangli Fan, Jingyun Wang* and Xiaojun Peng*

PTZ-Cy2 serves both as an absorbance ratiometric and a fluorescent "off-on" sensor for detecting hROS and gives a highly sensitive response to such endogenous species within the mitochondria of living cells.

779

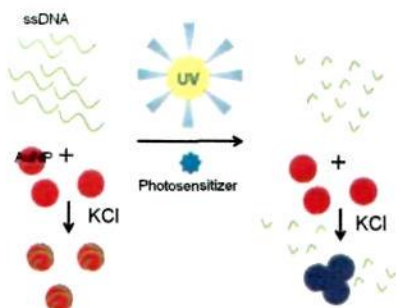


Utilizing modified flavonoids to construct a chemodosimeter array for discrimination of different palladium species by using principal component analysis

Yanxue Wang, Bin Liu,* Jiao Tian, Qianbiao Li, Fanfan Du, Taisheng Wang and Ruke Bai*

A simple chemodosimeter array has been successfully achieved for the detection and discrimination of different palladium species by using principal component analysis.

783



Colorimetric detection of UV light-induced single-strand DNA breaks using gold nanoparticles

Joong Hyun Kim, Chan Ho Chung and Bong Hyun Chung*

Salt-induced aggregation of gold nanoparticles was dependent on the size of single-strand DNA. As a result, breaking of the ssDNA by a photosensitizer under UV light irradiation could be detected by observing a red-to-purple color change of gold nanoparticles.

PAPERS

787



Subcellular spectroscopic markers, topography and nanomechanics of human lung cancer and breast cancer cells examined by combined confocal Raman microspectroscopy and atomic force microscopy

Gerald D. McEwen, Yangzhe Wu, Mingjie Tang, Xiaojun Qi, Zhongmiao Xiao, Sherry M. Baker, Tian Yu, Timothy A. Gilbertson, Daryll B. DeWald and Anhong Zhou*

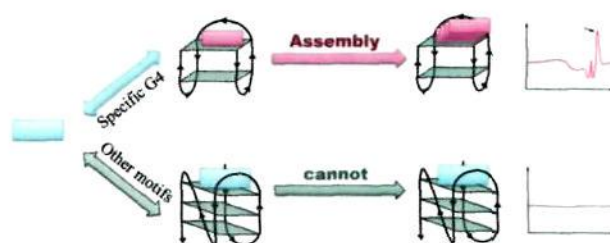
Novel application of Raman and AFM for the analysis of single cell mechanics, cytoarchitectures, and biochemical components of cancer cells.

798

A novel signal-amplified strategy based on assembly reactivation for highly specific and sensitive detection of chair-like antiparallel G-quadruplex

Wei Gai, Qianfan Yang,* Junfeng Xiang, Wei Jiang, Qian Li, Hongxia Sun, Lijia Yu, Qian Shang, Aijiao Guan, Hong Zhang and Yalin Tang*

A novel, signal-amplified strategy is proposed for highly specific and sensitive detection of G-quadruplex structures.

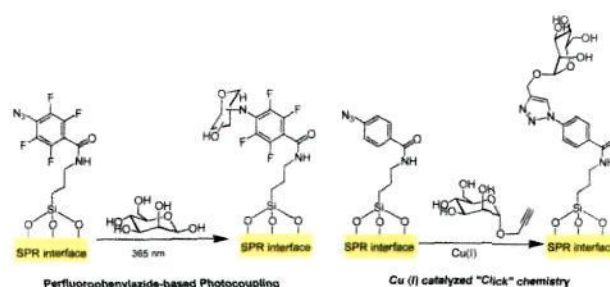


805

Comparison of photo- and Cu(I)-catalyzed "click" chemistries for the formation of carbohydrate SPR interfaces

Nazek Maalouli, Alexandre Barras, Aloysius Siriwardena, Mohamed Bouazaoui, Rabah Boukherroub and Sabine Szunerits*

The efficient coupling of glycans to SPR surfaces using "click" chemistry and photocoupling of underivatized glycans are compared.

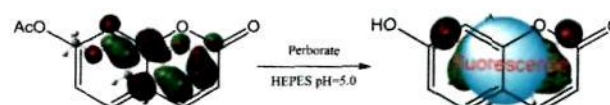


813

A highly selective fluorescent probe for BO_3^- based on acetate derivatives of coumarin in aqueous solution and thimerosal

Fangjun Huo, Long Wang, Yutao Yang, Yueyin Chu, Caixia Yin,* Jianbin Chao, Yongbin Zhang, Xuxiu Yan, Anmin Zheng,* Shuo Jin and Peng Zhi

We have employed 7-acetoxycoumarin for the design and construction of a new class of fluorometric assay to detect specifically the presence of perborate (BO_3^-) over a wide range of other anions in acetate buffered solution.

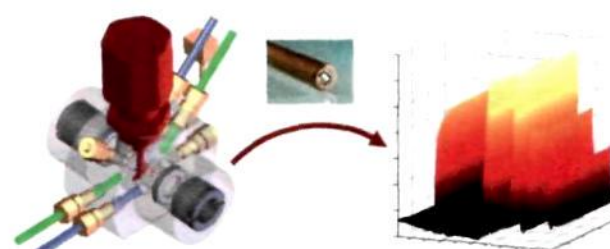


819

Comprehensive monitoring of a biphasic switchable solvent synthesis

Sonja Hardy, Irene M. de Wispelaere, Walter Leitner and Marcel A. Liauw*

A specially designed autoclave that allows simultaneous fibre-optic ATR IR and ATR UV-Vis measurements in both phases is used for quantitative analysis of a biphasic switchable solvent synthesis.

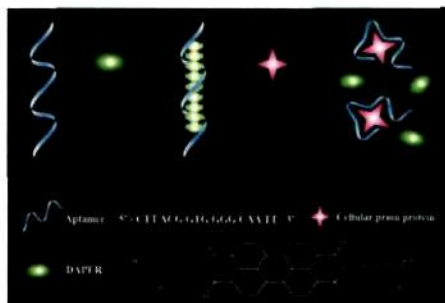


825

Aptamer-based spectrofluorometry for cellular prion protein using *N,N*-bis[3,3'-(dimethylamino)propylamine]-3,4,9,10-perylenetetracarboxylic diimide

Lei Zhan, Li Jiao Liang, Shu Jun Zhen, Chun Mei Li and Cheng Zhi Huang*

A label-free fluorescent aptamer probe for cellular prion protein (PrP^C) is reported based on the regulation of DAPER fluorescence, with comparable selectivity and sensitivity to other labelled PrP^C aptamer-based probes.

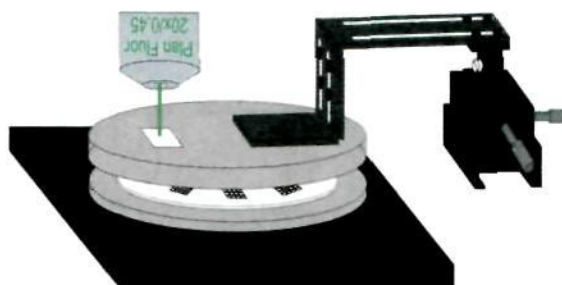


831

Laser-based directed release of array elements for efficient collection into targeted microwells

Nicholas C. Dobes, Rahul Dhopeswarkar, W. Hampton Henley, J. Michael Ramsey, Christopher E. Sims and Nancy L. Allbritton*

A cell separation strategy capable of the systematic isolation and collection of moderate to large numbers of single cells into a targeted microwell is demonstrated.

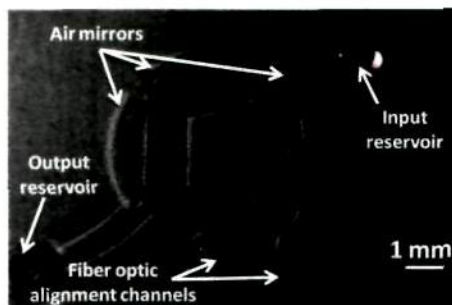


839

PDMS based photonic lab-on-a-chip for the selective optical detection of heavy metal ions

Bergoi Ibarlucea, César Díez-Gil, Inma Ratera, Jaume Veciana, Antonio Caballero, Fabiola Zapata, Alberto Tárraga, Pedro Molina, Stephanie Demming, Stephanus Büttgenbach, César Fernández-Sánchez and Andreu Llobera*

Feasible combination of inexpensive photonic lab-on-a-chip devices with ferrocene-based colorimetric ligands for the selective detection of Hg²⁺ and Pb²⁺.

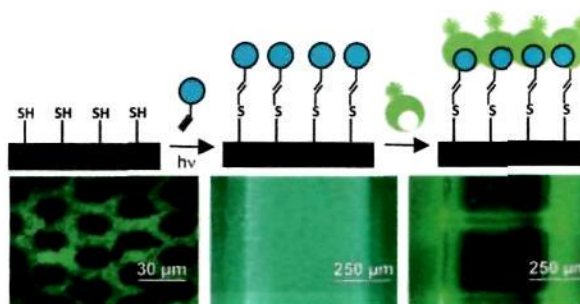


845

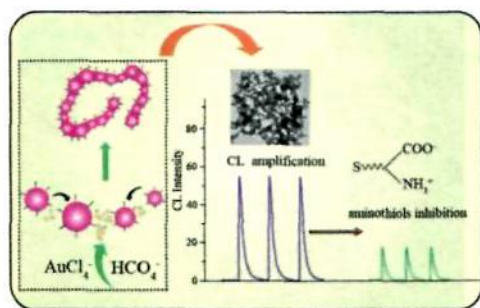
Rapid photochemical surface patterning of proteins in thiol-ene based microfluidic devices

Josiane P. Lafleur, Radoslaw Kwapiszewski, Thomas G. Jensen and Jörg P. Kutter*

This paper reports the rapid one-step photochemical surface patterning of biomolecules in microfluidic thiol-ene chips.



850

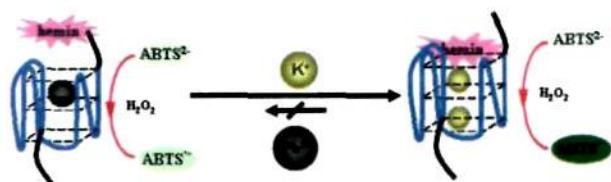


Chemiluminescence sensing of aminothiols in biological fluids using peroxymonocarbonate-prepared networked gold nanoparticles

Lijuan Zhang, Biqi Lu and Chao Lu*

We developed a facile approach to prepare the networked AuNPs by reactive oxygen species (HCO_4^-) reduction of HAuCl_4 in the presence of a fluorosurfactant. Such a novel material exhibited stronger CL activity and higher selectivity towards aminothiols than previously reported luminol–AuNP systems, and we have used this nanomaterial to sense aminothiols in human urine and plasma samples.

856

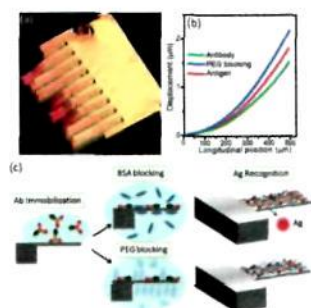


A novel colorimetric potassium sensor based on the substitution of lead from G-quadruplex

Huijiao Sun, Xiaohong Li,* Yunchao Li, Louzhen Fan and Heinz-Bernhard Kraatz*

A highly sensitive DNA sensor for colorimetric detection of K^+ based on substituting Pb^{2+} from G-quadruplex.

863

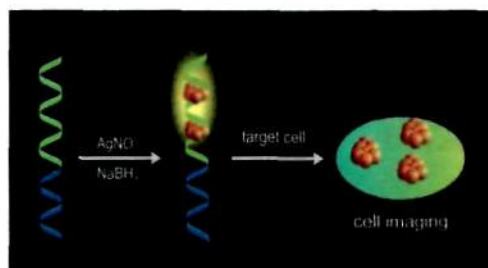


Tackling reproducibility in microcantilever biosensors: a statistical approach for sensitive and specific end-point detection of immunoreactions

Priscila M. Kosaka, Javier Tamayo,* José J. Ruz, Sara Puertas, Ester Polo, Valeria Grazu, Jesús M. de la Fuente and Montserrat Calleja

We develop here end-point detection with microcantilevers and achieve rates of true positives and true negatives of 90% and 91%, with a detection limit of 250 pM.

873



Effective detection and cell imaging of prion protein with new prepared targetable yellow-emission silver nanoclusters

Ya Wen Zhou, Chun Mei Li, Yue Liu and Cheng Zhi Huang*

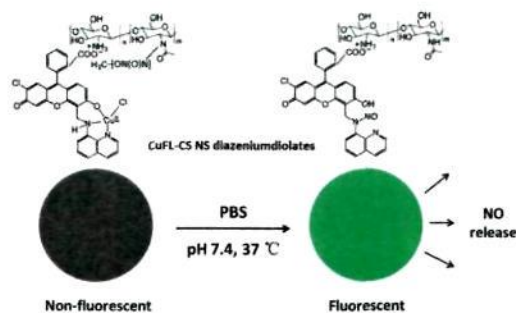
Highly selective detection and cell imaging of prion protein has been successfully developed by introducing targetable silver nanoclusters as a fluorescent probe.

879

Fluorescent chitosan complex nanosphere diazeniumdiolates as donors and sensitive real-time probes of nitric oxide

Lianjiang Tan, Ajun Wan* and Huili Li*

CuFL-CS NS diazeniumdiolates can release NO spontaneously in a PBS solution, and can meanwhile detect the release of NO with high sensitivity based on considerable fluorescence increase of the otherwise non-fluorescent nanosphere diazeniumdiolates caused by the released NO.

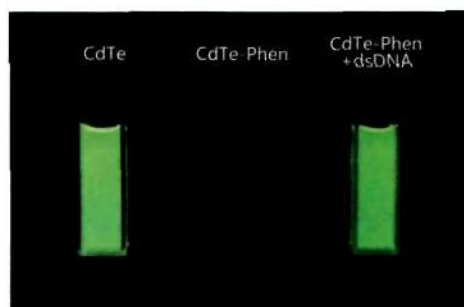


887

Quantum dot-phenanthroline dyads: detection of double-stranded DNA using a photoinduced hole transfer mechanism

Lu Zhang, Kao Zhu, Tao Ding, Xianyun Hu, Qingjiang Sun* and Chunxiang Xu

Sensitive detection of dsDNA by quantum dot-phenanthroline dyads operating with an "off-on" mode.

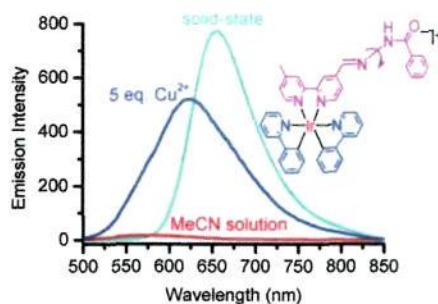


894

Aggregation-induced phosphorescence of iridium(III) complexes with 2,2'-bipyridine-acylhydrazone and their highly selective recognition to Cu²⁺

Na Zhao, Yu-Hui Wu, Jian Luo, Lin-Xi Shi and Zhong-Ning Chen*

Two cationic cyclometallated iridium(III) complexes with 2,2'-bipyridine-acylhydrazone show the aggregation-induced phosphorescence phenomenon and act as a significant 'off-on' luminescent switch for Cu²⁺.

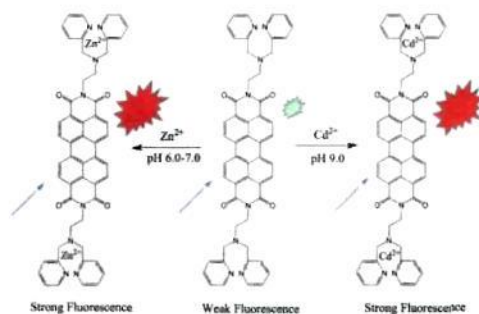


901

A turn-on fluorescent sensor for zinc and cadmium ions based on perylene tetracarboxylic diimide

Xiangjun Liu, Nan Zhang, Jin Zhou, Tianjun Chang, Canliang Fang and Dihua Shangguan*

A turn-on fluorescent probe, *N'*-bis-(*N,N*-di-(2-pyridylmethyl)-ethane-1,2-diamine)-perylene-3,4,9,10-tetracarboxylic diimide, which can respond to Zn²⁺ and Cd²⁺ respectively under different pH conditions.



907

Real-time electrochemical detection of pathogen DNA using electrostatic interaction of a redox probe

Minhaz Uddin Ahmed,* Sharifun Nahar, Mohammadali Safavieh and Mohammed Zourob*

We have established an immobilization free proof-of-principle using $[\text{Ru}(\text{NH}_3)_6]^{3+}$ for real-time electrochemical monitoring of a loop mediated isothermal amplification (LAMP) amplicon for target genes of *Escherichia coli* and *Staphylococcus aureus* by square wave voltammetry.



916

Molecular recognition and quantitative analysis of xylene isomers utilizing cataluminescence sensor array

Shaofang Li, Jianzhong Zheng, Wuxiang Zhang, Jing Cao, Shunxing Li and Zhiming Rao*

A novel method for the quantitative analysis of xylene isomers by sensor array based on nanomaterial Y_2O_3 , $\gamma\text{-Al}_2\text{O}_3$ and ZrO_2 (a-c) cataluminescence (CTL) combined with a least squares method is presented.

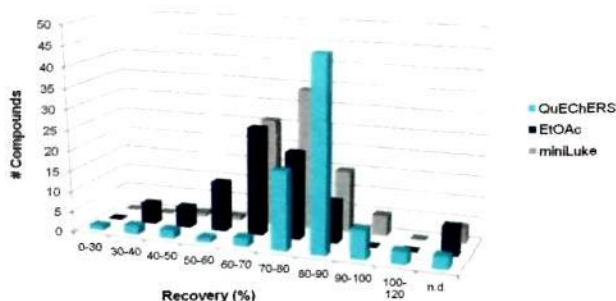


921

Comparison of three multiresidue methods to analyse pesticides in green tea with liquid and gas chromatography/tandem mass spectrometry

Łukasz Rajski, Ana Lozano, Noelia Belmonte-Valles, Ana Uclés, Samanta Uclés, Milagros Mezcua and Amadeo R. Fernandez-Alba*

This work compares three common multiresidue methods for tea analysis in terms of recovery, precision and amount of coextracted compounds.

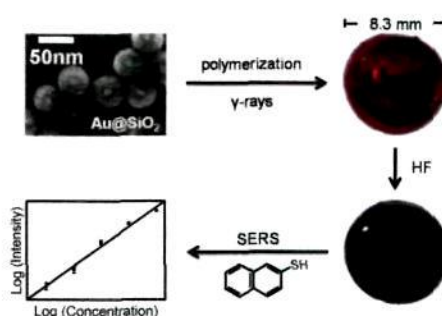


932

Au nanoparticle-encapsulated hydrogel substrates for robust and reproducible SERS measurement

Kayeong Shin, Kyungtag Ryu, Hoik Lee, Kwangsoo Kim, Hoeil Chung* and Daewon Sohn

A reliable and reproducible surface-enhanced Raman scattering (SERS) measurement utilizing Au nanoparticle-encapsulated hydrogels as a substrate has been demonstrated.

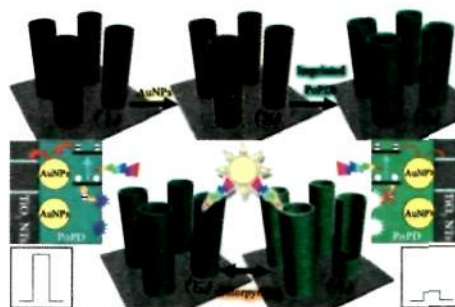


939

Visible light photoelectrochemical sensor based on Au nanoparticles and molecularly imprinted poly(*o*-phenylenediamine)-modified TiO₂ nanotubes for specific and sensitive detection chlorpyrifos

Panpan Wang, Weijian Dai, Lei Ge, Mei Yan, Shenguang Ge and Jinghua Yu*

A selective PEC sensor was fabricated on highly ordered, vertically aligned AuNPs-modified TiO₂ NTs, utilizing a molecularly imprinted poly(*o*-phenylenediamine) film as recognition element.

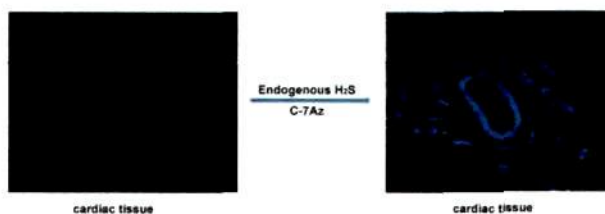


946

Fluorescent probe for highly selective and sensitive detection of hydrogen sulfide in living cells and cardiac tissues

Bifeng Chen, Wei Li, Cong Lv, Manman Zhao, Hongwei Jin, Hongfang Jin, Junbao Du, Liangren Zhang and Xinjing Tang*

H₂S visualization is successfully achieved in cells and cardiac tissues with a coumarin-based fluorescence probe.



952

Cyclohexanone and 3-aminopropyltrimethoxysilane mediated controlled synthesis of mixed nickel-iron hexacyanoferrate nanosol for selective sensing of glutathione and hydrogen peroxide

Prem Chandra Pandey* and Ashish Kumar Pandey

We report the cyclohexanone and 3-aminopropyltrimethoxysilane mediated controlled synthesis of mixed nickel-iron hexacyanoferrate nanosol of 34 nm average size.

